

Akzeptierter Artikel

Titel: The influence of distant substrates on the outcome of contact electrification

Autoren: Marta Siek, Witold Adamkiewicz, Yaroslav Sobolev, and Bartosz Grzybowski

Dieser Beitrag wurde nach Begutachtung und Überarbeitung sofort als "akzeptierter Artikel" (Accepted Article; AA) publiziert und kann unter Angabe der unten stehenden Digitalobjekt-Identifizierungsnummer (DOI) zitiert werden. Die deutsche Übersetzung wird gemeinsam mit der endgültigen englischen Fassung erscheinen. Die endgültige englische Fassung (Version of Record) wird ehestmöglich nach dem Redigieren und einem Korrekturgang als Early-View-Beitrag erscheinen und kann sich naturgemäß von der AA-Fassung unterscheiden. Leser sollten daher die endgültige Fassung, sobald sie veröffentlicht ist, verwenden. Für die AA-Fassung trägt der Autor die alleinige Verantwortung.

Zitierweise: *Angew. Chem. Int. Ed.* 10.1002/anie.201806658
Angew. Chem. 10.1002/ange.201806658

Link zur VoR: <http://dx.doi.org/10.1002/anie.201806658>
<http://dx.doi.org/10.1002/ange.201806658>

The influence of distant substrates on the outcome of contact electrification**

Marta Siek[†], Witold Adamkiewicz[†], Yaroslav I. Sobolev[†], Bartosz A. Grzybowski*

Abstract. *Magnitudes of charges developed on contact-electrified polymers depend not only on the properties of these materials but also on the nature of distant substrates on which the polymers are supported. In particular, image charges induced in conductive substrates can reduce charges on the polymers by arc discharge through the surrounding gas. This mode of charge dissipation occurs on time scales of milliseconds and can be prevented by insulating the sharp edges of the conductive supports.*

Contact electrification is a process in which two materials are brought together (with or without friction) and then separated to produce charges of net opposite polarity on the contacting surfaces.^[1] Although CE has been studied since the antiquity^[2] and is used in numerous important technologies (photocopying and laser printing,^[3] electrostatic painting,^[4] industrial separations,^[5] triboelectric generators^[6]) it is still incompletely understood, especially between pairs of insulating materials. Recent years have witnessed a revival of interest in the fundamental aspects of CE between insulators – with the help of modern surface characterization techniques, it has been possible to establish that electrification entails creation of both charges and radicals,^[7a-c] produces microscopic (+/-) charge “mosaics” on each of the contacting surfaces,^[7d] is accompanied by the transfer of miniscule amounts of materials,^[7e,f] and can occur not only between different but also identical materials.^[7g] Two common assumptions in all these and many other^[1a,b,d,8] studies have been that (i) CE is a surface phenomenon with all the relevant processes limited to within, at most, 60 nm from the insulator’s surface^[9] and (ii) the maximal magnitude of the developed charges is limited by the dielectric breakdown of the gas between the charging surfaces. On the other hand, it should be remembered that contact-charged interfaces also produce electric fields and can induce image charges far away from the interfacial region. In the widely studied triboelectric generators, such image charges are created in grounded conductive substrates and are rapidly (within μ s) harnessed to into electrical current.^[6] When, however, the substrates are not grounded, new channels of charge dissipation can become operative on longer time scales. Here, we show how such dissipation of induced/image charges “feeds back” and modifies the distribution of surface charges on the

initially electrified polymers. As a consequence of this “feedback,” the magnitudes of net charges measured on the polymers depend on the conductivity of substrates that were never in contact with the charge-separating interface. As we show, these effects can be attributed to the locations and dynamics of the discharge of gas not between the contact-charging surfaces – which, as mentioned above is well documented^[10] – but between the distant substrate and these surfaces. We also demonstrate how the discharges can be eliminated without adjusting the dielectric strength of the gas, by insulating the substrate’s edges. Overall, these findings extend our understanding of CE beyond the properties of the contacting materials and can help systematize^[11] the study of this interesting and important phenomenon.

Figure 1a illustrates experimental arrangement in which a block/“stamp” of poly(dimethylsiloxane) (PDMS, $w = 10$ mm, $l = 10$ mm, $h = 6$ mm) was placed on and then peeled off a polymer film deposited by spin-coating on some other material. PDMS was used as a stamp material because it is known to come into conformal contact with other polymers.^[7d,7g,13a,b] The spin-coated polymers used here were poly(methyl methacrylate) (PMMA, MW=350k, Sigma-Aldrich), poly(vinyl acetate) (PVAc, MW=500k, Sigma-Aldrich), polyvinylpyrrolidone (PVP, MW=50k, Alfa Aesar), and poly(4-vinylphenol) (PVPh, MW=25k, Sigma-Aldrich). These choices were motivated not only by the desire to survey different chemical structures but also the fact that PMMA and PVAc are well known electrets^[10a] (i.e., materials capable of generating internal and external electric fields) whereas PVP and PVPh are not. As we shall see, the results were qualitatively similar for electrets and non-electrets. The polymers were deposited on substrates covering a wide range of resistivities – from single crystal copper (volume electrical resistivity $1.7 \times 10^{-8} \Omega\cdot\text{m}$), through various types of silicon ($2.4 \times 10^{-5} - 1.0 \times 10^1 \Omega\cdot\text{m}$), to highly-oriented pyrolytic graphite ($5.0 \times 10^{-3} \Omega\cdot\text{m}$), sapphire ($1.0 \times 10^{13} \Omega\cdot\text{m}$), borosilicate glass ($1.0 \times 10^{14} \Omega\cdot\text{m}$), mica ($1.0 \times 10^{15} \Omega\cdot\text{m}$), and quartz ($1.0 \times 10^{15} \Omega\cdot\text{m}$) (for further details, see SI, **Table S1**). In most experiments described below, the film thickness was $\sim 1 \mu\text{m}$ though the results were similar for thicknesses ranging from $\sim 0.5 \mu\text{m}$ – $5.5 \mu\text{m}$ (see **Figure S5**). Relative humidity, RH, was typically $\sim 24\%$ but experiments at $\sim 50\%$ and 80% were also performed. In all cases, the temperature was $\sim 23^\circ\text{C}$, the stamps were left in contact with the substrate for 45 min prior to peeling off, and the pressure of contact was ~ 37 Pa (see SI, Section 2). The net charges developed on the stamp and on the polymer film/substrate composite Q were measured by a home-made Faraday cup connected to a Keithley 6517B high-precision electrometer.

The key results of these studies are summarized in **Figures 1b-e** which plot mean surface charge densities, σ (i.e., net charges Q measured by the electrometer divided by the area of stamp/film contact) developed on the films (solid markers) and on the PDMS stamps (open markers) as a function of the substrate’s resistivity. As seen, for low-resistivity substrates, σ is close to zero ($\sim 1 \text{ pC}\cdot\text{cm}^{-2}$); for high-resistivities, the values of σ are scattered around $3 \text{ nC}\cdot\text{cm}^{-2}$. For the stamps, the dependence on the substrate’s resistivity is not as pronounced, but the values of σ recorded in experiments with polymer

[*] Dr. Marta Siek, Dr. Witold Adamkiewicz, Dr. Yaroslav Sobolev, Prof. B.A. Grzybowski
IBS Center for Soft and Living Matter and
Department of Chemistry, UNIST,
50, UNIST-gil, Eonyang-eup, Ulsan-gun, Ulsan, South Korea
E-mail: nanogrzybowski@gmail.com

[**] Authors gratefully acknowledge generous support from the Institute for Basic Science Korea, Project Code IBS-R020-D1. The authors gratefully acknowledge Dr. Marcin Holdyński and Dr. Pavel Bakharev for their help with XPS analyses.

[†] Authors contributed equally

Supporting information for this article is available on the WWW under <http://dx.doi.org/10.1002/anie.201xxxxx>.

films on low-resistivity supports are still $\sim 7.3\text{--}35.7\%$ lower than the ca. $-3 \text{ nC}\cdot\text{cm}^{-2}$ values recorded when highly resistive supports were used.

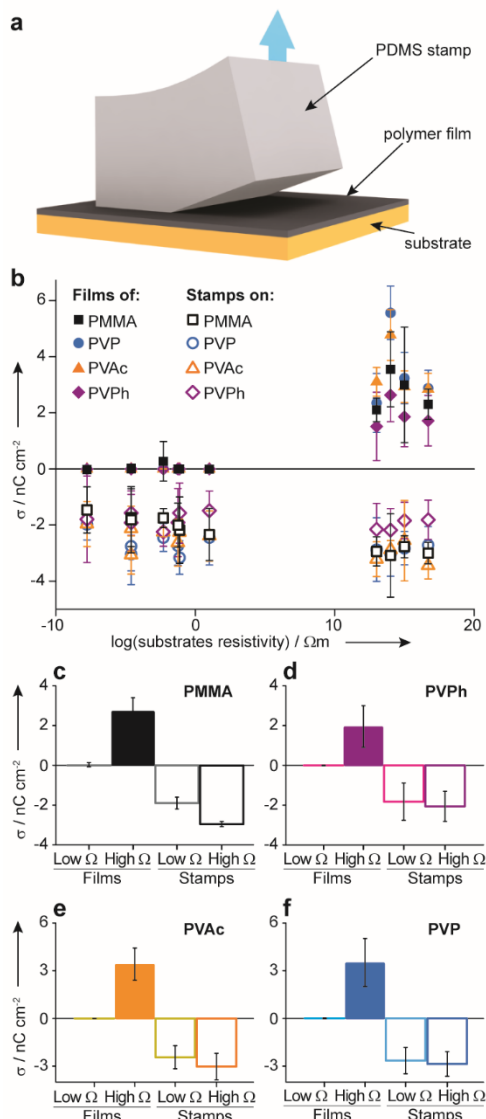


Figure 1. Net charges developed on contact-electrified insulators depend on the resistivity of a distant substrate. **a)** Scheme of the experimental arrangement comprised of a $10\times 10\times 6 \text{ mm}$ PDMS stamp applied onto and peeled-off a polymer film (typically, $1 \mu\text{m}$ thick) spin-coated on a $15\times 15\times 0.3 \text{ mm}$ substrate. **b)** Net charge density on the polymer/substrate films (full markers) and the PDMS stamp (open markers) plotted as a function of the resistivity of the underlying substrates. Scale bars are standard deviations based on $N = 7$ independent experiments (each with a freshly prepared stamp/film/substrate system). **c–f)** Same raw data as in (b) but with the mean charge densities averaged over substrates grouped as „Low Ω “ if resistivity was below $7 \Omega\cdot\text{m}$ and „High Ω “ if it was above $7 \Omega\cdot\text{m}$. Each panel is for a different polymer in the film: (c) PMMA, (d) PVPh, (e) PVAc, (f) PVP.

Interestingly, the maximal magnitudes of σ on highly-resistive substrates coincide with the $\sim 3\text{nC}\cdot\text{cm}^{-2}$ value^[10a] required for the electrical breakdown of air between uniform and oppositely charged planes. To investigate the role of breakdown, we performed CE experiments under the atmosphere of SF_6 (whose dielectric strength is twice that of air in 0.5 mm gaps or thrice in 5 mm gaps^[10b]). For substrates with high resistivity, the results were as expected – namely, the density of surface charges increased with increasing dielectric strength of the gas (Figure 2a). With less resistive substrates,

however, the net charges developed on the polymer films/substrates were close to zero for all gasses (Figure 2b) – that is, were, again, pointing to the importance of the substrate itself and not only the gas.

Next, if the conductive substrate was grounded through the electrometer during the delamination (vs. being introduced into the Faraday cup after the delamination), the charge recorded by the electrometer was not zero and increased with increasing dielectric strength of the gas (Figure 2c). This result means that over time-scales of drainage to the ground ($< 0.1 \mu\text{s}$), the charge was present on the system – but in the absence of grounding, it somehow dissipated by another channel and over a longer time scale.

In search of this additional dissipation channel, one may consider discharge through a thin layer of water adsorbed on the electrified surface. While this scenario^[9f] can account for the lack of charge on relatively hydrophilic films (water contact angles $\sim 70^\circ$) on non-conductive, “High Ω ” substrates at RH $\sim 80\%$, it cannot explain why for RH up to $\sim 50\%$, the same films on “High Ω ” substrates retain charge whereas those on “Low Ω ” substrates show no net charge (compare left vs. right panels in Figure 2d; note also that hydrophobic surfaces of PDMS stamps do not discharge irrespective of RH value, for further discussion see Section 3e of the SI). Also, the differences in the measured charges cannot be attributed to surface-chemical effects – indeed, as evidenced by XPS and TOF-SIMS analyses described in the SI Section 3f, the compositions of electrified films supported by conductive vs. insulating supports are almost indistinguishable.

Given these results, we decided to image the CE process directly using the ultra-low-light detection system (the HNü 512 TEC-cooled EMCCD camera, Nüvü, Canada, with a PMS-12LC5M lens, $N_A=0.3$). Figure 2d shows a typical outcome of these experiments with a low resistivity substrate (here, for a PMMA film on a p-type, B-doped silicon, $6.5\times 10^{-2} \Omega\cdot\text{m}$). The image clearly shows a discharge arc^[10g,h] originating from the edge of the substrate and penetrating into the region between the PDMS and PMMA being separated.

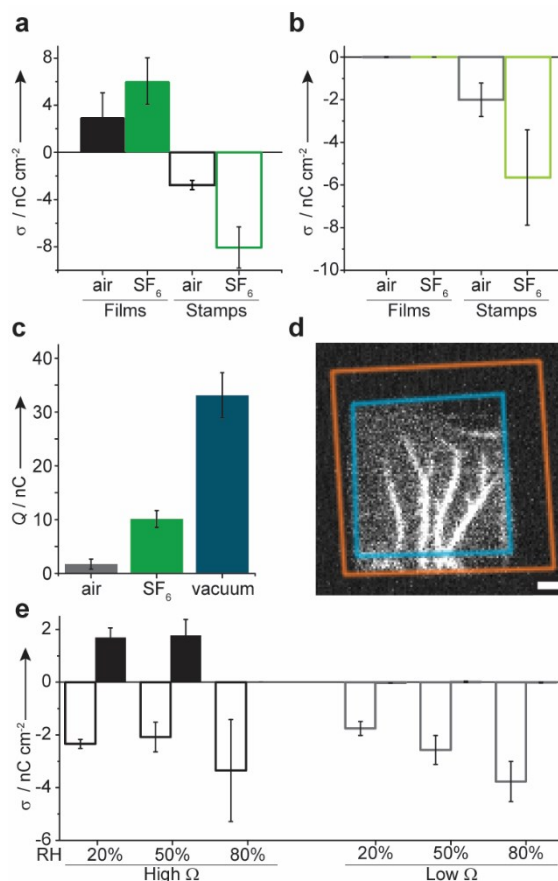


Figure 2. The influence of the surrounding gas and substrate grounding and visualization of electrical discharge. **a)** When the substrate supporting the polymer film (here, 1 μm PMMA) is highly-resistive (here, mica), the net charges developed on both the stamp and the film increase with the dielectric strength of the gas (here, air and SF_6). **b)** If the substrate is conductive, the dependence of gas properties is observed only for the stamp whereas for the film the net charge is zero irrespective of the gas. **c)** When, however, the conductive substrates are grounded through electrometer during stamp delamination, the charge harnessed from the substrates is non-zero and increasing with gas' dielectric strength (here, air, SF_6 , and 10^{-2} mbar vacuum (dielectric strength 35 times that of air in 0.5 mm gaps, or 15 times that of air in 5 mm gaps^[13c-f]). Error bars in (a-c) are based on three independent experiments. **d)** High-sensitivity camera image of the arc discharge observed during delamination of a PDMS stamp (blue outline) from 1- μm -thick PMMA supported on p-type, B-doped Si (orange outline). The substrate was not grounded. Scale bar represents 2 mm. Exposure time was 300 ms. **e)** Charges on PDMS stamps (open bars) and on PMMA films (solid bars) supported by "High- Ω " mica (left panel) and "Low Ω ," p-type B-doped Si (right panel).

Importantly, the discharge arcs are not observed when the perimeter of the low-resistivity substrate is covered with a layer of non-conductive material (e.g., 2-mm thick ethylene-vinyl acetate, Superbonder DT-12, $\epsilon_r = 2.8$, dielectric strength seven times that of air). Schemes and data in **Figures 3a** and **3b** directly compare the surface charge densities measured for the same films (PMMA) and conductive substrates (p-type, B-doped silicon, $6.5 \times 10^{-2} \Omega\cdot\text{m}$) but with vs. without the insulating layer along the edges of the substrate. When these edges are insulated, the magnitudes of σ on both the stamp and the film are higher than without insulation. Taken together, these results directly prove that discharge from the edges of a conductive (but ungrounded) substrate is the main channel of charge loss.

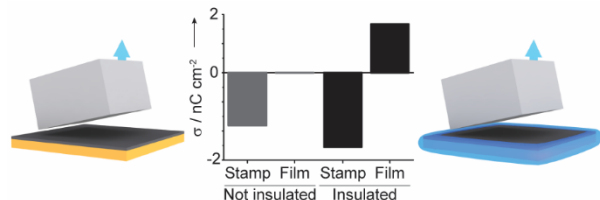


Figure 3. Schemes of the experiments (sides) and charge densities (middle) for contact-charging of PDMS against 1 μm -thick PMMA films supported on conductive p-type, B-doped silicon, $6.5 \times 10^{-2} \Omega\cdot\text{m}$ with free edges of the substrate (left, gray markers) and with the edges covered with 2-mm thick layer of ethylene-vinyl acetate (right, black markers).

With the above experimental evidence at hand, we are now in position to provide theoretical interpretation of the observed phenomena. Assume for now that the polymeric film and the substrate are infinite (**Figure 4a**). In this infinite-flat-charged-plane approximation, surface charge density σ_1 on the top surface of the polymer creates a uniform electric field of magnitude $\sigma_1/2\epsilon$ in a medium with permittivity ϵ . Since the field in the conductor must be at all times zero, the conductive substrate polarizes to cancel the external field. Consequently, its upper surface will have the free charge surface density σ_2 and the lower surface, density $\sigma_3 = -\sigma_2$ due to electroneutrality of the substrate before the ignition of gas discharges. From zero-field condition in the conductor ($(\sigma_1 + \sigma_2 - \sigma_3)/2\epsilon = 0$) it follows that $\sigma_3 = -\sigma_2 = \sigma_1/2$. Gas discharges disrupt the electroneutrality of the substrate and die out only when electric field in the gas diminishes ($(\sigma_1 + \sigma_2 + \sigma_3)/2\epsilon \approx 0$), which results in $\sigma_3 = 0$, $\sigma_2 = -\sigma_1$, and zero field everywhere except the polymer. In reality, the system is not infinite and the conductor is limited by its edges. For such a case, finite-element calculations (**Figure 4b**) show, as expected, that the density of charges at the edges/corners is higher than over the flat regions. In fact, for the

surface charge densities we measure ($\sim 3 \text{ nC}\cdot\text{cm}^{-2}$) the field strength at these locations is as high as $27 \text{ MV}\cdot\text{m}^{-1}$ – that is, much higher than the threshold value for dielectric breakdown of air (marked with a dashed line in **Figure 4b**) or any other gas at atmospheric pressure. As the breakdown from these regions takes place, the distribution of charges in the system changes but, as before, the ultimate charge configuration maintains the zero field inside of the conductive support (see scheme in **Figure 4c** and the FEM-calculated field distribution in **Figure 4b**).

It should be emphasized that even though the final net charge of the polymer/substrate pair is zero (as σ_1 and σ_2 compensate each other; cf. **Figure 4c**), the above scenario prescribes that the charges created by CE at the polymer's top surface are not dissipated after discharge. This can be tested by measuring the potential directly above the polymer film with respect to the potential of the substrate – potential should be constant everywhere above the film and equal to $((\sigma_1 + \sigma_2)/2\epsilon_1)d = (\sigma_1/\epsilon_1)d$, where d is the film thickness. For typical discharge-limited value $\sigma_1 = 3 \text{ nC}\cdot\text{cm}^{-2}$ and $d = 1 \mu\text{m}$, this formula predicts 0.94 V. Indeed, KPFM imaging of the center of PMMA film on silicon substrate after stamping with PDMS showed an potential with average value of 0.92 V (see **Figure S28**), providing an experimental verification of the model.

When the substrate is an insulator having dielectric constant ϵ_2 , image charges in the substrate are weaker by a factor of $(\epsilon_2 + \epsilon_1)/(\epsilon_2 - \epsilon_1)$. For example, for PMMA ($\epsilon_1 = 3.6$) on quartz ($\epsilon_2 = 4.5$) this factor is 9, and fields at the corners are weakened proportionally. More importantly, even if corona discharge ignites in this case, it can discharge, at most, 1/9 of the total charge. Additionally, regions of high field span less than 0.1 mm (see SI, **Figure S27**), and since dielectric strength of gases is higher in a more confined field (e.g. for air, dielectric strength is 3-10 times higher in 0.1-0.01 mm gaps than in 1 mm gaps^[10a, 13c]), discharges are further inhibited.

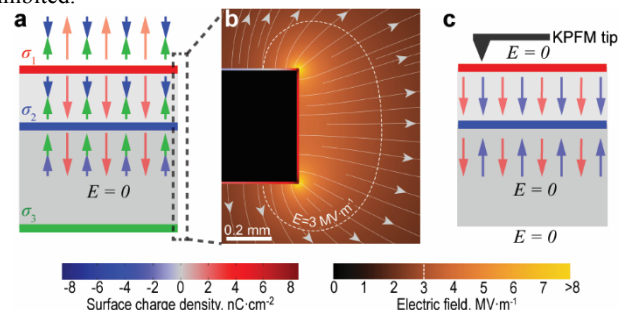


Figure 4. **a)** Scheme illustrating electrostatic fields in a polymer film and a conductive substrate beneath (both approximated as infinite-planes) after CE but before any discharge. Arrows show contributions to electric field from charge density on the top surface of the polymer film (red), surface of conductive substrate directly under the polymer (blue) and the opposite side of conductive substrate (green). **b)** Numerically calculated electric field and charge density on substrate's surfaces for the same materials but with finite spatial extent. Charge density on the polymer film is not shown. Notice the zero field inside conductor and higher charge densities near the corners. Field in the region outlined by the dashed line exceeds breakdown strength of air ($3 \text{ MV}\cdot\text{m}^{-1}$). **c)** Scheme analogous to (a) but after discharge.

Finally, we consider why the charge on the stamp also diminishes if the polymer film is supported by a conductive substrate. We note that the polarities of the stamp and the image charges discharging from the substrate are opposite – it is therefore plausible to assume that the spark originating from the substrate is directed towards and affects (i.e., partly discharges) the stamp's surface. In fact, the tree-like pattern of discharge is imprinted into the stamp and is clearly visualized when, right after CE, the stamp is sputtered with toner particles attracted to the charged regions of the surface^[14] (**Figure 5a**). Interestingly, even when discharges from the corners of the substrate are eliminated by dielectric cladding, final charge

densities on both the stamp and the polymer film (e.g., $-2.55 \text{ nC}\cdot\text{cm}^2$ on PDMS and $1.67 \text{ nC}\cdot\text{cm}^2$ on PMMA) are slightly lower than the corresponding values obtained in experiments with dielectric substrates (-2.95 and $2.74 \text{ nC}\cdot\text{cm}^2$, respectively). This indicates that in addition to discharge from the substrate's edges, there must exist a second mechanism by which substrate's conductivity influences final charge densities. Indeed, finite-element calculations of the electric field during stamp delamination (**Figure 5b**) reveal that the field magnitude in the region shown in **Figure 5c** – close to the point of stamp detachment – reaches breakdown threshold at 15%–30%^[15] lower charge densities if the substrate is conductive, in qualitative agreement with the observed difference. This modulation of electric field in the stamp-film gap originates from the interplay of electrostatic reflection of both the charged stamp and the charged polymeric film in the conductive substrate and the conservation of substrate's electroneutrality.

In summary, we have shown that image charges induced in distant conductive supports can feed-back and dissipate the original charges developed by CE on contacting insulators. We suggest that in order to ensure reproducibility of data, any future reports of CE should include detailed information about the underlying substrates even if these substrates seem to be distant and not participating in the CE process.

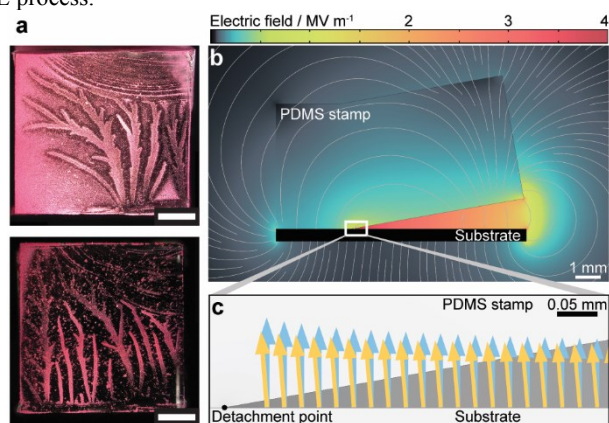


Figure 5. Influence of the substrate on the charging of the stamp. **a)** Distribution of charge on $1\times 1 \text{ cm}$ PDMS stamps visualized by toner particles. Tree-like patterns are due to discharges originating from the edge of the substrate (compare to the spark shown in Figure 2d). **b)** Electrostatic field during the process of stamp detachment, as calculated using the finite elements method. Field lines are shown in grey. Color scale indicates the magnitude of electric field. **c)** Zoom of the region near the point of stamp detachment. Blue arrows = calculated electric field in the air gap when the substrate under the PMMA film is conductive. Yellow arrows = field in the same gap and for the same charge density generated during CE but for the case of a non-conductive substrate (quartz, $\epsilon_r = 4.5$).

Received:

Published online on:

Keywords: Contact electrification, electric fields, gas discharge

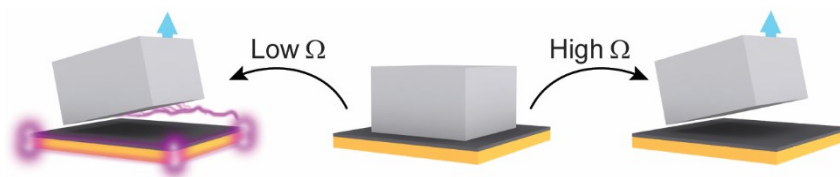
- [1] a) W. R. Harper, *Contact and Frictional Electrification*, Laplacian Press, Morgan Hill, CA, **1998**; b) R.G., Horn, D.T. Smith, A. Grabbe, *Nature* **1993**, *366*, 442–443; c) J. Lowell, A.C. Rose-Innes, *Adv. Phys.* **1980**, *29*, 947–1023; d) D. J. Lacks, R. M. Sankaran, *J. Phys. D: Appl. Phys.* **2011**, *44*, 453001; e) L. S. McCarty, G. M. Whitesides, *Angew. Chem. Int. Ed.* **2008**, *47*, 2188–2207; f) F. Galembeck, T. A. L. Burgo, L. B. S. Balestrin, R. F. Gouveia, C. A. Silva, A. Galembeck, *RSC Adv.* **2014**, *4*, 64280–64298.
- [2] a) P. F. O'Grade *Thales of Miletus: The Beginnings of Western Science And Philosophy*, Aldershot, UK, **2002**; b) W. Gilbert, *De Magnete*, Vol. 2 (Ed.: P. Short), London, **1600**; c) J. Wilcke, *Philos. Trans. R. Soc. London* **1759**, *11*, 401; d) A. Volta, *Proc. R. Soc. London* **1800**, *1*, 27–29; e) A. Volta, *Philos. Trans. R. Soc. London* **1800**, *90*, 403–431; f) M. Faraday, *Experimental Researches in Electricity*, Vol. 2, R. & J. E. Taylor, London, **1843**, pp. 2075–2145;

- [3] a) J. W. Weigl, *Angew. Chem. Int. Ed.* **1977**, *16*, 374–392; b) J. W. Weigl, *Angew. Chemie* **1977**, *89*, 386–406; c) D. M. Pai, B. E. Springett, *Rev. Mod. Phys.* **1993**, *65*, 163–211; d) H. O. Jacobs, S. A. Campbell, M. G. Steward, *Adv. Mater.* **2002**, *14*, 1553–1557.
- [4] a) W. Kleber, B. Makin, *Part. Sci. Technol.* **1998**, *16*, 43–53; b) A. G. Bailey, *J. Electrostat.* **1998**, *45*, 85–120.
- [5] a) A. Tilmatine, S. Bendimerad, M. Younes, L. Dascalescu, *Int. J. Sustain. Eng.* **2009**, *2*, 184–191; b) M. J. Pearse, M. I. Pope, *Powder Technol.* **1977**, *17*, 83–89.
- [6] a) S. Wang, L. Lin, Z. L. Wang, *Nano Lett.* **2012**, *12*, 6339–6346; b) Y. Zhu, B. Yang, J. Liu, X. Wang, L. Wang, X. Chen, C. Yang, *Sci. Rep.* **2016**, *6*, 22233; c) Z. H. Lin, G. Cheng, L. Lin, S. Lee, Z. L. Wang, *Angew. Chem., Int. Ed.* **2013**, *52*, 12545–12549; d) F. R. Fan, Z. Q. Tian, Z. L. Wang, *Nano Energy* **2012**, *1*, 328–334; e) S. Wang, Y. Xie, S. Niu, L. Lin, C. Liu, Y. S. Zhou, Z. L. Wang, *Adv. Mater.* **2014**, *26*, 6720–6728; f) G. Zhu, W. Q. Yang, T. Zhang, Q. Jing, J. Chen, Y. S. Zhou, P. Bai, Z. L. Wang, *Nano Lett.* **2014**, *14*, 3208–3213; g) J. Wang, C. Wu, Y. Dai, Z. Zhao, A. Wang, T. Zhang, Z. L. Wang, *Nat. Commun.* **2017**, *8*, 88; h) A. Li, Y. Zi, H. Guo, Z. L. Wang, F. M. Fernandez, *Nat. Nanotechnol.* **2017**, *12*, 481–487.
- [7] a) B. Baytekin, H. T. Baytekin, B. A. Grzybowski, *J. Am. Chem. Soc.* **2012**, *134*, 7223–7226; b) H. T. Baytekin, B. Baytekin, T. M. Hermans, B. Kowalczyk, B. A. Grzybowski, *Science* **2013**, *341*, 1368–1371; c) T. Mazur, B. A. Grzybowski, *Chem. Sci.* **2017**, *8*, 2025–2032; d) H. T. Baytekin, A. Z. Patashinski, M. Branicki, B. Baytekin, S. Soh, B. A. Grzybowski, *Science* **2011**, *333*, 308–312; e) W. R. Salaneck, A. Paton, D. T. Clark, *J. Appl. Phys.* **1976**, *47*, 144; f) H. T. Baytekin, B. Baytekin, J. T. Incorvati, B. A. Grzybowski, *Angew. Chem., Int. Ed.* **2012**, *124*, 4927–4931; g) M. M. Apodaca, P. J. Wesson, K. J. M. Bishop, M. A. Ratner, B. A. Grzybowski, *Angew. Chem., Int. Ed.* **2010**, *49*, 946–949.
- [8] a) C. Liu, A. J. Bard, *Nat. Mater.* **2008**, *7*, 505–509; b) C. Y. Liu, A. J. Bard, *J. Am. Chem. Soc.* **2009**, *131*, 6397–6401; c) C. Y. Liu, A. J. Bard, *Chem. Phys. Lett.* **2010**, *485*, 231–234.
- [9] a) W. J. Brennan, J. Lowell, M. C. O'Neill, M. P. W. Wilson, *J. Phys. D: Appl. Phys.* **2000**, *25*, 1513–1517; b) P. K. Watson, Z.-Z. Yu, *J. Electrostat.* **1997**, *40–41*, 67–72; c) S. L. Burkett, E. M. Charlson, E. J. Charlson, H. K. Yasuda, *J. Appl. Polym. Sci.* **1996**, *61*, 47–56; d) K. P. Homewood, *J. Phys. D: Appl. Phys.* **1984**, *17*, 1255; e) J.A. Wiles, B.A. Grzybowski, A. Winkleman, G.M. Whitesides, *Anal. Chem.* **2003**, *75*, 4859–4867; f) J.A. Wiles, M. Fialkowski, M.R. Radowski, G.M. Whitesides, B.A. Grzybowski, *J. Phys. Chem. B* **2004**, *108*, 20296–20302.
- [10] a) G. M. Sessler, in *Electrets* (Ed.: G.M. Sessler), Springer-Verlag, Berlin, Heidelberg, **1987**, pp. 13–80; b) J. M. Meek, J. D. Craggs, *Electrical Breakdown of Gases*, John Wiley And Sons, Chichester, U.K., **1978**; c) L. S. McCarty, A. Winkleman, G. M. Whitesides, *J. Am. Chem. Soc.* **2007**, *129*, 4075–4088; d) S. Soh, S. W. Kwok, H. Liu, G. M. Whitesides, *J. Am. Chem. Soc.* **2012**, *134*, 20151–20159; e) P. M. Ireland, *J. Electrostat.* **2009**, *67*, 462–467; f) R. G. Horn, D. T. Smith, *Science* **1992**, *256*, 362–364; g) B.V. Derjaguin, N.A. Krotova, *Usp. Fiz. Nauk*, **1948**, *36*, 387–406; h) B.V. Derjaguin, N.A. Krotova, *Adhesion Publishers of Akad. Nauk SSSR*, Moscow, **1949**.
- [11] Historically, the study of CE between insulators have been marred by conflicting reports of apparently the same bulk materials exhibiting markedly different characteristics. Several such observations were ascribed to interfacial effects (chemisorption in ref [1b], surface reaction in [9e]; humidity-driven surface reorganization in [9f]), but the majority of discrepancies remain unexplained (see ref [9e] and references therein). Part of the problem might be that the substrates supporting the polymers are generally not reported in sufficient detail (e.g., p-type silicon^[12]).
- [12] a) J. J. Cole, C. R. Barry, R. J. Knuesel, X. Wang, H. O. Jacobs, *Langmuir* **2011**, *27*, 7321–7329; b) H. O. Jacobs, S. A. Campbell, M. G. Steward, *Adv. Mater.* **2002**, *14*, 1553–1557.
- [13] a) D. C. Duffy, J. C. McDonald, O. J. A. Schueller, G. M. Whitesides, *Anal. Chem.* **1998**, *70*, 4974–4984; b) A. Perl, D. N. Reinhoudt, J. Huskens,

- Adv. Mater.* **2009**, *21*, 2257-2268; c) T. W. Dakin, G. Luxa, G. Oppermann, J. Vigreux, G. Wind, H. Winkelkemper, *Electra* **1974**, *32*, 61-82; d) M. J. Mulcahy, P. C. Bolin, *High Voltage Breakdown Study. Handbook of Vacuum Insulation*, Ion Physics Corporation, Burlington, MA, **1971**; e) N. Zouache, A. Lefort, *IEEE Trans. Dielect. Electr. Ins.* **1997**, *4*, 358-364; f) D. Lyon, A. Hubler, *IEEE Trans. Dielect. Electr. Ins.* **2013**, *20*, 1467-1471.
- [14] M. W. Williams, *AIP Advances* **2012**, *2*, 010701
- [15] This range of calculated values originates from the dependence of electrostatic field on the angle between the stamp and the film during the process of detachment. We estimated that in our experiments this angle is usually between 3 and 15 degrees, but varies from sample to sample. This angle also changes during the act of delamination itself.

Contact electrification

Marta Siek, Witold Adamkiewicz,
 Yaroslav I. Sobolev and Bartosz A.
 Grzybowski*



Not only the surface matters in contact electrification. Image charges induced in distant conductive supports (Low Ω) can feed-back and dissipate the original charges developed by CE on contacting insulators.